



Published in final edited form as:

Mech Ageing Dev. 2020 October ; 191: 111351. doi:10.1016/j.mad.2020.111351.

Functional recreation of age-related CD8 T cells in young mice identifies drivers of aging- and human-specific tissue pathology

Akanksha Panwar^{a,1}, Michelle Jhun^{a,1}, Altan Rentsendorj^a, Armen Mardiros^{a,2}, Ryan Corder^{a,b}, Kurtis Birch^a, Nicole Yeager^{a,b}, Gretchen Duvall^a, David Golchian^a, Maya Koronyo-Hamaoui^{a,b}, Robert M. Cohen^c, Eric Ley^{f,2}, Keith L. Black^a, Christopher J. Wheeler^{a,g,h,3,*}

^aDept. Neurosurgery, Maxine Dunitz Neurosurgical Institute, Cedars-Sinai Medical Center, 8700 Beverly Blvd., Los Angeles, CA 90048, United States

^bDep. Biomedical Sciences, 8700 Beverly Blvd., Los Angeles, CA, 90048, United States

^cDept. Psychiatry & Behavioral Sciences and Neuroscience Program, GDBBS, Emory University, 201 Dowman Dr., Atlanta, GA 30322, United States

^fDept. Surgery, 8700 Beverly Blvd., Los Angeles, CA, 90048, United States

^gBrain Mapping Foundation, Society for Brain Mapping & Therapeutics, 860 Via De la Paz, Pacific Palisades, CA 90272, United States

^hT-Neuro Pharma, 1451 Innovation Parkway SE, Albuquerque, NM 87123, United States

Abstract

Mitigating effects of aging on human health remains elusive because aging impacts multiple systems simultaneously, and because experimental animals exhibit critical aging differences relative to humans. Separation of aging into discrete processes may identify targetable drivers of pathology, particularly when applied to human-specific features. Gradual homeostatic expansion of CD8 T cells dominantly alters their function in aging humans but not in mice. Injecting T cells into athymic mice induces rapid homeostatic expansion, but its relevance to aging remains uncertain. We hypothesized that homeostatic expansion of T cells injected into T-deficient hosts models physiologically relevant CD8 T cell aging in young mice, and aimed to analyze age-related T cell phenotype and tissue pathology in such animals. Indeed, we found that such injection

This is an open access article under the CC BY-NC-ND license (<http://creativecommons.org/licenses/by-nc-nd/4.0/>).

*Corresponding author at: P.O. Box 781, Aptos, CA 95001, United States, Chris@TNeuroPharma.com, chris.wheeler@brainmappingfoundation.org (C.J. Wheeler).

²Present address: Kite Pharma, 2400 Broadway, Santa Monica, CA 90404.

³Present address: Brain Mapping Foundation, Society for Brain Mapping & Therapeutics, 860 Via De La Paz, Suite E-1, Pacific Palisades, CA 90272; T-Neuro Pharma, 1451 Innovation Parkway SE, Suite # 600, Albuquerque, NM 87123; P.O. Box 781, Aptos, CA 95001.

¹These authors contributed equally to the manuscript.

Declaration of Competing Interest

C. Wheeler is the author of patents PCT/US2016/049598, WO 2017/040594 and PCT/US2019/017879. R. Corder and K. Black are co-authors on patent PCT/US2019/017879. PCT/US2016/049598, WO 2017/040594 is licensed by Cedars-Sinai Medical Center to T-Neuro Pharma, Inc. C. Wheeler has ownership interest in T-Neuro Pharma, Inc.

Appendix A. Supplementary data

Supplementary material related to this article can be found, in the online version, at doi:<https://doi.org/10.1016/j.mad.2020.111351>.

conferred uniform age-related phenotype, genotype, and function to mouse CD8 T cells, heightened age-associated tissue pathology in young athymic hosts, and humanized amyloidosis after brain injury in secondary wild-type recipients. This validates a model conferring a human-specific aging feature to mice that identifies targetable drivers of tissue pathology. Similar examination of independent aging features should promote systematic understanding of aging and identify additional targets to mitigate its effects on human health.

Keywords

CD8 T cell; Resident memory T cell; Cellular immunity; Homeostatic expansion; Neurodegeneration; Immune aging

1. Introduction

One of the central unanswered questions in biology is how aging leads to coordinated dysfunction in multiple tissues throughout the body. Related to this is how aging increases susceptibility to tissue pathology. The complexity and pervasiveness of aging across multiple bodily systems underlies this conundrum. In addition, critical aspects of aging differ substantially between the experimental rodent systems widely used to study them, and humans. To identify discrete targetable features of age-related tissue pathology, and relevance to human health, there is thus a critical need to deconvolute aging into separable components, as well as render it more human-like in experimental rodent systems. Current health-related aging research focuses on cellular senescence, yet some aspects of aging are initiated upon sexual maturity, and as such predate the onset of cellular senescence by years or decades. Examining these earliest age-related processes may reap the most substantial benefits in any effort to deconvolute aging.

While accumulation of senescent cells is thought to contribute to age-related pathologies, immune dysfunction, particularly within the cytolytic (CD8) T cell compartment, can occur completely separate from aging or time-dependent cellular senescence (Zlamy et al., 2016). Shortly after puberty, an aberrant subpopulation of phenotypically and functionally distinct memory CD8 T cells begins to progressively accumulate in the circulation, partially in response to thymic involution (Zlamy et al., 2016; LeMaoult et al., 2000; Messaoudi et al., 2006). This subpopulation exhibits age-related changes in homing to tissues including brain in both humans and mice, and expresses markers of resident-memory CD8 T cells (CD8 T_{RM}) (Park and Kupper, 2015; Wakim et al., 2012; Smolders et al., 2013; Ritzel et al., 2016; Rodriguez-Garcia et al., 2018). In the circulation, age-related CD8 T_{RM} become prominent by middle age in most individual people, and can promote immune-mediated tissue damage upon re-stimulation (Clambey et al., 2005, 2008; den Braber et al., 2012; Schwab et al., 1997). As such, CD8 T_{RM} accumulation is a prime candidate to coordinate the breakdown of multiple tissues during aging. Nevertheless, the impact of this phenomenon on tissue pathology outside the immune system itself is poorly understood, in large part because it is not easily studied in experimental rodents.

In contrast to humans where they dominantly overtake the T cell pool in aging, the impact of CD8 T_{RM} expansion in mice is offset by compensatory factors including continual

production of new T cells by the thymus (Clambey et al., 2005; den Braber et al., 2012). Hence, expanded CD8 TRM exhibit a relatively minor influence on the mouse T cell pool even at advanced ages (den Braber et al., 2012). Moreover, and as with most age-related phenomena, CD8 TRM accumulation also occurs simultaneously with all other age-related changes in humans and in mice. Thus, determining its impact on aging pathology is problematic without models to examine it in isolation. Such models would ideally mimic the impact of CD8 TRM expansion in humans to be most informative for human health. To achieve this, we considered the physiological causes of age-related CD8 TRM expansion.

Age-related accumulation of CD8 TRM is dependent on homeostatic expansion. This ordinarily occurs gradually as production of new CD8 T cells progressively wanes over time, and existing CD8 T cells begin to expand in response to available antigens, refilling the depleted T cell niche. Rapid homeostatic expansion of T cells also occurs when T cells are introduced into hosts that intrinsically lack a full T cell niche (athymic or lymphocyte-deficient strains), but the relevance of this inducible age-independent phenomena to age-related CD8 TRM expansion and age-related disorders has not been examined. We hypothesized that homeostatic expansion in T-deficient hosts models physiologically relevant CD8 T cell aging in young mice, and conducted phenotypic and physiological studies to test this. Specifically, we examined age-related T cell phenotype in nude hosts injected with CD8 T cells, as well as examine age-related tissue pathology in such mice, most notably in brain with and without accompanying injury.

We established that inducible homeostatic expansion of CD8 T cells by injection into athymic mouse hosts (nude; B6.Foxn1) mimics the molecular, phenotypic, and functional properties of aberrant age-related CD8 TRM with 100 % penetrance. We therefore examined the resulting homeostatically-induced- or ^{hi}TRM-bearing mice for evidence of tissue pathology in skin and brain, and their role in “humanizing” distinct pathological responses in mice.

Our findings strongly suggest that age-dependent accumulation of CD8 TRM is accurately modeled by inducible homeostatic expansion of CD8 T cells in young mice. Additionally, CD8 TRM in these mice mediated coordinated damage to multiple tissues including skin and brain, that were reminiscent of aging. Finally, CD8 TRM elicited human-specific molecular pathology in response to brain trauma, essentially eliminating a clinical disparity between mice and humans. Our model represents a reductionist model to study the role of a discrete component of aging separate from others, that promises to illuminate not only aspects of age-related immune dysfunction, but targetable drivers of age-related pathology in distinct tissues such as skin and brain.

2. Methods

2.1. Animal subjects

Female C57BL/6, B6.Foxn1 mice, and congenic and/or syngeneic knockout strains (Jackson Labs) were housed in a pathogen-free vivarium under standard conditions on a 12-h light/12-h dark cycle with food and water *ad libitum*. Recipient animals were 8–10 week-old female C57BL/6, B6.Foxn1 (B6.Cg-Foxn1^{nu}/J), or B6.Foxn1/AppKO mice; donors were 5–

8 week-old C57BL/6 or B6.CD45.1-congenic (B6.CD45.1-Cg; B6.SJL-*Ptprc*^a*Pepc*^b/BoyJ), B6.Prf-KO (Perforin1-deficient; C57BL/6-*Prf1*^{tm1Sdz/J}), or B6.Ifng-KO (Ifng-deficient; B6.129S7-*Ifng*^{tm1Ts/J}) females. B6.45-1-congenic, B6.Foxn1/AppKO and B6.Foxn1 mice were all backcrossed onto wild-type C57BL/6 backgrounds for ≥ 14 generations at Jackson Labs, and are thus syngeneic by their operational criteria. Cell derivation was randomized by pooling from ≥ 5 donors per experiment. Young (8–10 wk) and aged (15 months) male and female C57BL/6 mice ($n = 12$ young; $n = 7$ –8 aged) were used. Donor, recipient, and unmanipulated animals were maintained in a pathogen-free facility under the Cedars-Sinai Department of Comparative Medicine, with all breeding and genetic screening conducted at Jackson Laboratories (Bar Harbor, ME).

2.2. Adoptive transfer of CD8 T cells

Splenic CD8⁺ T cells from C57BL/6 J or CD45.1-Cg female mice (5–8 weeks old) were purified using anti-CD8 immunobeads (Miltenyi Biotech, Sunnyvale, CA). 3×10^6 CD8 T cells in 50 μ l of PBS were injected i.v. into female C57BL/6 J or B6.Foxn1 nude hosts. Transfer efficiency into B6.Foxn1 hosts was validated by persistence of ≥ 5 % CD8⁺ T cells within splenic lymphocytes 3 weeks after injection. The order of treatments was randomized by alternating cell and control injections between individual recipients. For all subsequent analyses, performing investigators were blinded to both group definition and anticipated outcomes. B6.Foxn1 and C57BL/6 are both CD45.2. CD45.1-congenic (B6.SJL-*Ptprc*^a*Pepc*^b/BoyJ) donors were used when injecting C57BL/6 recipients to discern donor from other CD8 T cells. Both CD45.1 and CD45.2 (wild-type C57BL/6) donors were used when injecting B6.Foxn1 recipients, and yielded identical results and trends (not shown). Phenotype, genotype, and pathological results are all from CD45.1 (C57BL/6) CD8 T cell donors unless otherwise stated.

2.3. CFSE labeling of lymphocytes

CD8 T cells were labeled with CFSE dye according to manufacturer's instructions (CellTrace CFSE Cell Proliferation Kit C34554; Molecular Probes). Briefly, 5–10 μ M dye was used to stain affinity-purified CD8 T cells. To maintain normal cellular physiology and reduced potential artifacts from overloading, the concentration of dye was kept as low as feasible. Reagent preparation: a 5 mM CellTrace CFSE stock solution was prepared immediately prior to use by dissolving the contents of one vial in 18 μ L of DMSO (provided in kit). 2 μ l of 5 mM stock CFSE solution was added per ml cells (1 – 2×10^7 cells/mL) for a final working concentration of 10 μ M, followed by incubation at 37°C for 10 min. Staining was quenched by adding 5 volumes of ice-cold culture media to the cells, followed by 5 min incubation on ice, and centrifugation. Cells were then washed by resuspending the pellet in fresh media, repeated two more times for a total of three washes. Flow cytometric analysis of adoptive transferred CFSE-labeled cells was performed with 488 nm excitation and emission filters appropriate for fluorescein.

2.4. Tissue processing (brain, spleen)

Brains and spleens were harvested from PBS-perfused mice. Brains were sectioned 1 mm to the right of the longitudinal fissure (midline). For single-cell suspensions, brains were removed with blood-free surgical instruments, passed through 45 μ m nylon mesh,

centrifuged at $600 \times g$, and pellets retained. 1 mL ultra-pure H₂O was added to the pellet, followed by 20 mL of 2% FBS/PBS within 2 s for additional RBC lysis. Pellets were centrifuged at $600 \times g$, and pellets resuspended in 10 mL of 2% FBS/PBS, which was subsequently passed through a 22 G needle 2x, then through a 25 G needle 2x, and finally through a 30 G needle 2x, with needle changes as necessary. Live lymphocytes were counted after trypan blue staining for flow cytometry.

For brain cell lysates used in protein studies, right hemispheres were flash frozen in $-80 \text{ }^{\circ}\text{C}$ conditions, followed by homogenization in Cell Lysis Buffer (Cell Signaling Technologies, MA), and centrifugation of nuclei. Cell lysates were separated into Triton soluble, Sarkosyl soluble and Sarkosyl insoluble fractions using sequential incubations of 10 % (wt/V) salt sucrose solution and 1 % (wt/v) sarkosyl Salt Sucrose Solution. Left hemispheres fixed in 4 % paraformaldehyde and reserved for immunohistochemical staining. Brain Weight standardization: Upon removal of whole brain from cranium, cerebellum, brainstem, and olfactory bulbs were removed prior to weighing on a Mettler balance.

2.5. TCR V β D-J joint PCR analysis

D β to J β rearrangements were analyzed as previously described (Aifantis et al., 1997; Gärtner et al., 1999). Briefly, DJ β 1 recombination products were detected using the forward and reverse primers:

D β -5'-Primer

TCRB-D1U-S GAGGAGCAGCTTATCTGGTGGTTT

TCRB-D2U-S GTAGGCACCTGTGGGAAGAAACT

J β -3'-Primer

TCRB-J1D-A CACAACCCCTCCAGTCAGAAATG

TCRB-J2D-A TGAGAGCTGTCTCCTACTATCGATT

Primers amplifying the IgM constant region, IgM-FWD (5'CACTAGCCACACCCCTTAGCAC3') and IgM-REV (5'TGGCCATGGGCTGCCTAGCCCGGACTT3'), were used as an amplification control. Brain and spleen genomic DNA was isolated as previously described (LeMaout et al., 2000). 1 μg of brain genomic DNA or 10 ng of spleen genomic DNA were used to template the PCRs containing 1 μM each primer, 0.25 mM each dNTP, 2 mM Mg^{2+} , 1X PCR buffer (Invitrogen), 1 U Platinum Taq polymerase in 20 μl total volume. The PCR cycling conditions were: 5 min at $94 \text{ }^{\circ}\text{C}$ followed by 36 cycles of 45 s at $94 \text{ }^{\circ}\text{C}$, 90 s at $65 \text{ }^{\circ}\text{C}$ and 150 s at $72 \text{ }^{\circ}\text{C}$ followed by a final extension at $72 \text{ }^{\circ}\text{C}$ for 10 min. The run-off products were loaded onto agarose gels for size separation, stained with ethidium bromide, and presence of individual allele bands quantified by fluorescence intensity scans. For final analysis, equal amounts of material was loaded onto gels based on equivalent IgM C region PCR product per sample, which was assumed to reflect comparable cell content. Percentage of individuals

expressing each allele were compiled from ≥ 4 (middle-aged brain only) or ≥ 10 (all others) individual biological replicates per group.

2.6. Western blot

Triton-soluble cell lysates were electrophoretically separated on 12 % Tris-HCl Precast Gels (Bio-Rad), and blotted onto 0.2 μm nitrocellulose. Membranes were blocked with BSA, incubated in sequential primary and secondary antibody dilutions for 1 h at room temperature with ≥ 3 washes, developed with enhanced chemiluminescence substrate (GE Healthcare Biosciences; Pittsburgh, PA), and exposed onto Amersham Hyperfilm (GE Healthcare Biosciences; Pittsburgh, PA).^{22,88}

2.7. ELISA

Supernatant from homogenized brain tissues was used for Triton-soluble A β . Insoluble pellets from Triton-homogenized brain were resuspended in 10 volumes 5 M Guanidine HCl 4 h to generate Guanidine-soluble A β . Triton- and Guanidine-soluble samples were subjected to analysis by Soluble and Insoluble A β ELISA (Invitrogen, Life Technologies; Grand Island, NY). Absorbance was read on a SPEC-TRAmix Plus384 microplate reader (Molecular Devices, Sunnyvale, CA) with data analyzed in Graphpad PRISM (Graphpad Software; San Diego, CA).

2.8. Flow cytometry

Purified T cells stained with respective Abs were analyzed by three-color flow cytometry (FACScan II; BD Biosciences, San Jose, CA) to assess purity. Antibodies were incubated with whole-spleen single cell suspension in PBS with 5 % FBS, on ice for 30 min, followed by a wash with the PBS with 5 % FBS. 100,000–300,000 flow events were acquired. Gating and compensation was set using fluorochrome- and isotype-matched controls on each tissue and sample type, with gates drawn to exclude ≥ 99.9 % of unstained cells for each fluorochrome, and compensation adjusted to exclude >99.9 % of double-stained cells in controls. Gates and compensation were maintained as constant for each antibody stain combination and analysis.

2.9. Antibodies for tissue staining and western blots

Free-floating brain sections (8–14 μm thick) were mounted onto slides and blocked for 1 h at RT. Sections were incubated at 4 $^{\circ}\text{C}$ overnight with primary antibody in blocking solution (Dako, CA). Sections were rinsed 4x in PBS, and incubated 90 min in fluorochrome- or biotin-conjugated secondary antibody (0.01 % in PBS). Sections were washed, coverslipped, and mounted with ProLongGold anti-fade media with DAPI (Invitrogen). Bright-field and fluorescent images were obtained using a Zeiss AxioImagerZ1 with CCD camera (Carl Zeiss Micro imaging). Image analysis of micrographs was performed with ImageJ (NIH). Anti-pTau pS199/202 antibody (Invitrogen) was used at 1:50 for IHC and 1:100 for WB, with PHFs confirmed with Phospho-PHF-tau pSer202+Thr205 Antibody (AT8), used at 1:2000 for WB. Due to marker size, pTau WB signal was normalized to that of β -actin (clone AC-74, Sigma), with GAPDH used for normalization of all other markers. Anti-GFAP (Dako) was used at 1:250 for IHC and WB. Anti-NeuN antibody (Chemicon) was

used at 1:100 for IHC and WB. Anti-Iba1 (Wako, Ltd.) was used at 1:200 for IHC. Anti-CD8 (clones 53–6.72 and 2.43, BD Pharmingen) was used at 1:100 for IHC and 1:1000 for WB, respectively. All secondary antibodies (HRP, Alexa Flour-488, –594, –647; Invitrogen) were used at 1:200 for IHC and 1:2000 for WB. Multimer generation & use: dextramers of established epitopes for self/brain antigen (Trp-2-DCT_(180–188)/H-2K^b), and/or custom APP epitopes with predicted affinities < 100 nM (NetMHC version 3.4), were manufactured by Immudex.

2.10. CD8 T cell purification & injection

C57BL/6 J or B6.CD45.1-congenic (B6.SJL-*Ptprc^a Pepc^b*/BoyJ) CD8 T cells were purified by MACS anti-CD8 affinity column, and injected into B6.Foxn1 at 3×10^6 , i.v.. For secondary CD8 T cell transfer, spleens were harvested from ^{hi}T-B6.Foxn1 donors after in vivo expansion (3–4 weeks later). Resulting pe-expanded CD8 T cells were similarly purified by MACS affinity column, and 6–10 week old female C57BL/6 J recipient mice injected with 3×10^6 purified cells, i.v.. Presence of donor T cells in C57BL/6 J recipients was determined 3 and 10 wk later by flow cytometry on blood, and confirmed by Western blot and IF at 6 and 15 months. Genotypes: C57BL/6 (B6); B6.CD45.1-congenic; B6.Foxn1 (2° donor & recipient); C57BL/6 (recipients).

2.11. Pigmentation analysis

Wild-type (C57BL/6 J female) CD8 T cells were purified by MACS affinity column, and either these cells (3×10^6) or PBS was injected i.v. into 10 week old B6.Foxn1 female hosts. Presence of donor T cells was determined 3 and 10 wk after injection by flow cytometry on blood, and with terminal examination 15 months after injection. Total pigmentation around face, inguinal regions, and extremities scored on a 0–10 scale with the highest score equal to the most highly pigmented (typically PBS-injected donors), and the lowest (0) indicating no visibly discernible pigmentation. Genotypes: C57BL/6 (B6; hosts); B6.Foxn1 (recipients).

2.12. Traumatic brain injury

Ten-week-old wild-type female C57BL/6 mice of similar size were anesthetized with isoflurane, the left frontoparietal shaved, and individual mice placed in a stereotaxic frame. Injury directly to the left frontoparietal skull will be delivered using the Impact One Stereotaxic Impactor (MyNeuroLab, St. Louis, MO) for closed cortical impact with the following settings: 2-mm piston tip, 3-m/s impact velocity, 30-millisecond dwell time, and 3-mm impact depth. Sham mice were similarly placed into the stereotaxic frame, without impact delivery. Time to movement from supine to prone was recorded during recovery, and mice with times > 12 min excluded from analysis (typically due to non-recovery).

2.13. Statistical analysis

Quantification and stereological counting procedure for cell numbers or area (μm^2) of Amyloid beta plaque, GFAP⁺, Iba1⁺ or Perforin1⁺ cells were analyzed in six to eight coronal sections from each individual, at 150- μm intervals (unless otherwise indicated), covering 900–1200 μm of the hippocampal and cortical areas. Specific fluorescence signal was captured with the same exposure time for each image and optical sections from each field of

the specimen were imported into NIH Image J and analyzed as above. GraphPad Prism (version 5.0b; San Diego, CA, USA) was used to analyze the data using ANOVA and T-Tests with Welch's correction (no assumption of equal variance). In all histograms, average \pm SEM is depicted.

Sample sizes for PrfKO-CD8 and Ifn γ KO-CD8 groups were calculated *a priori* for each metric using means and standard deviations of PBS and wt-CD8 groups for anticipated effect sizes, with alpha 0.05, and >95 confidence. Calculated n plus ≥ 1 were then used for PrfKO-CD8 and Ifn γ KO-CD8 groups.

Pre-determined exclusions included sections or samples with no discernible background signal, and values within each group ≥ 2 standard deviations above or below the mean/group. Subject numbers and methods of reagent validation are shown in Table S1.

2.14. Study approval

All animal procedures were approved prior to performance by the Cedars-Sinai Institutional Animal Care and Use Committee.

3. Results

3.1. Uniform induction of “hiT” cells in nude mice

CD8 T cells from young (<9 wk) C57BL/B6 (B6) donors, CD45.1-congenic B6, or B6 donors with effector gene knockout (PrfKO or IfngKO) were injected into B6.Foxn1 recipients to examine the role of CD8 T cell pro-inflammatory and lytic function on homeostatic expansion and related sequelae. Where warranted (i.e., in wild-type B6 recipients injected with CD45.1-congenic CD8 T cells), lymphocytes were gated for donor surface marker CD45.2 by flow cytometry where appropriate, and evaluated for peripheral expansion (Fig. 1A, B). B6 CD8 T cells were also injected into young nude hosts lacking the Amyloid Precursor Protein gene (B6.Foxn1/AppKO) to examine the possible role of App as a promoters of tissue-specific inflammation in modulating donor cell expansion [Puig et al., 2017, 2012]. Donor CD8 T cells injected in young B6.Foxn1 recipients (CD8 \rightarrow B6.Foxn1 respectively) expanded within 8 days regardless of donor effector gene knockout and remained in circulation. Donor CD8 T cells injected into young B6.Foxn1/AppKO also expanded within 8 days (Fig. 1C). By contrast, CD8 T cells serially transferred from nude recipients back into wild-type B6 or B6.CD45.2-congenic hosts (CD8 \rightarrow B6.Foxn1 \rightarrow B6) did not expand (Fig. 1C). As expected, CD8 T cells labeled with the cytoplasmic dye, CFSE, prior to injection into B6.Foxn1 hosts exhibited the laddered dye dilution and population enlargement typical of homeostatic expansion within 4 days (Fig. 1D). This early expansion was delayed, however, in B6.Foxn1/AppKO recipients (Fig. 1D), suggesting that the earliest phase of homeostatic expansion may be dependent on reactivity to a self App epitope. Unfortunately, B6.Foxn1/AppKO hosts were about a third the size of either parental strain and did not survive more than a few weeks, and so did not contribute to further analyses.

3.2 ^{hi}T and aged CD8 T cell phenotype, genotype, function

Analysis of homeostatically-induced donor CD8 T cells (“^{hi}T” cells) in B6.Foxn1 hosts by flow cytometry revealed a surface marker profile identical to CD8 T cells undergoing clonal expansion in aged mice (CD122^{hi}, CD127^{hi}, CD44^{hi}, KLRG1^{hi}, PNA^{hi}, CD8^{lo}, CD103⁺; Fig. 2A–D) (LeMaoult et al., 2000; Messaoudi et al., 2006; Clambey et al., 2005, 2008; Messaoudi et al., 2004). A similar phenotype is found on CD8 T cell clonal expansions in aging humans (Clambey et al., 2005). The T cell markers CD44 and KLRG1 establish that these homeostatically induced, or “^{hi}T” cells belong to a memory T cell subset associated with aging (Clambey et al., 2008), while CD103 expression is further characteristic of resident-memory CD8 T cells, or T_{RM} (Mackay et al., 2012; Gebhardt and Mackay, 2012). Nevertheless, resident-memory T cells normally reside in peripheral non-immune tissues, although they can migrate into the general circulation as “ex-T_{RM}” (Fonseca et al., 2020). Since in our model, these cells appear to arise within the circulation, we thus regard them as “pre-TRM” cells when observed in the general circulation/spleen, but more generally refer to them as “homeostatically-induced” or “^{hi}T cells” in recipient mice, unless they are within non-immune tissues

Age-related expansion decreases clonal diversity of CD8 T cells (LeMaoult et al., 2000; Schwab et al., 1997; Messaoudi et al., 2004; Ahmed et al., 2009; Degauque et al., 2011; Morley et al., 1995; Posnett et al., 1994, 2003; Ricalton et al., 1998; Buchholz et al., 2011). We thus sought to quantify ^{hi}T clonality. To do this, we analyzed variable region D→J rearrangements in T Cell Receptor beta gene segments by PCR from brain, as previously described (Aifantis et al., 1997; Gärtner et al., 1999). This methodology provides a measure of overall clonal diversity T cells without extensive sequencing data from each individual TCR V region/joint as in TCR spectratyping, by detecting productive TCRβ D-J joints. These DNA recombination events are required for the generation of a productive TCR and for T cell maturation. The methodology is additionally insensitive to the propensity of tissue-resident CD8 T cells to undergo apoptosis upon tissue dissociation (Wakim et al., 2010), as well as to brain autofluorescence that can complicate flow cytometric analysis (Duong and Han, 2013). We thus determined the proportion of biological replicate brain samples using each of the detectable 12 D-J joints. Consistent with previous reports, splenic T cells in wild-type mice aged 12 months showed minimal clonal skewing in TCRVβ, whereas those injected into nude recipients exhibited both D1→J1 and D2→J2 clonal skewing after just 10 weeks (Supplemental Fig. S1). Increasing D1→J1 and D2→J2 clonal skewing was most evident, however, in brains of middle-aged (6 months) and aged (>12 months) wild-type mice (Fig. 2E–G, Supplemental Fig. S1). These cohorts exhibited progressive reduction of D→J diversity with age in brain, whereas D→J usage in young wild-type mouse brain exhibited substantial diversity (Fig. 1E, F). D→J joints in brains of young ^{hi}T-bearing nude mice also exhibited reduced diversity similar to that of aged mice (Fig. 2E), and D→J segment usage in these as well as aged mice were both significantly different from that in young mice (Fig. 2F, Supplemental Fig. S1). Indeed, D→J segment usage in brains of young ^{hi}T-bearing nude hosts was most similar to that in aged wild-type mice (Fig. 1G).

TCR V β D \rightarrow J joint analysis strongly suggested that ^{hi}T reside in brain. We thus examined presence, phenotype, and antigen reactivity of ^{hi}T cells in brain more directly by flow cytometry and Western blot analysis. CFSE-labeled donor CD8 T cells injected into B6.Foxn1 hosts were found increased in brain parenchyma three days later, confirming rapid localization of ^{hi}T cells to brain (Fig. 3A, B). CD8 protein on brain Western blots was also increased in both nude ^{hi}T recipients 10 weeks after injection, and in aged relative to young wild-type mice (Fig. 2C), suggesting similar functional localization to brain in ^{hi}T-bearing nudes and affected aged mice (Ritzel et al., 2016). Although overall levels of CD8 T cells in brain appeared similar to wild-type by flow cytometry, this likely reflected sensitivity to tissue dissociation (Wakim et al., 2010). Qualitatively, however, flow cytometry revealed that IFN γ ⁺ and KLRG1⁺ CD8 T cells that retained CD103 expression were significantly increased in ^{hi}T_{RM}-bearing nude brains (Fig. 3D). Unexpectedly high apoptosis of lymphocytes derived from brains of aging mice prohibited direct comparison by flow cytometry. Nevertheless, multiple studies have documented that resident memory CD8 T cells in aging tissues including brain and others, express CD103, and up-regulate both KLRG1 and pro-inflammatory cytokines including IFN γ (Ritzel et al., 2016; Clambey et al., 2008; Onyema et al., 2012; Schenkel et al., 2013). Thus, ^{hi}T cells in nude brain phenotypically correspond to typical CD8 T_{RM} within aging tissues. This altered T cell population was also evident in the periphery, as KLRG1⁺ CD8 T cells reactive to MHC I-restricted antigens including Tyrosinase-related Protein-2/Dopachrome Tautomerase (Trp-2/DCT_[180–188]) and APP_[470–478] were expanded in blood, corroborating host T cell expansion dynamics in B6.Foxn1/AppKO hosts (Fig. 1D; 3 E, F). Nevertheless, only APP-reactive CD8 T_{RM} were significantly increased in brain (Fig. 3E, F). Thus, ^{hi}T cells reactive to two distinct self antigens expanded peripherally in nude hosts, whereas those reactive to an APP epitope selectively accumulated in brain.

3.3. Skin de-pigmentation in ^{hi}T-bearing nude mice

Given that a significant portion of ^{hi}T cells were reactive to the brain/skin antigen, Trp-2, it was notable that ^{hi}T-bearing B6.Foxn1 hosts exhibited reduction in pigmentation relative to PBS-injected controls at 15 months (Fig. 4A–C). Moreover, while brain weight in ^{hi}T-bearing B6.Foxn1 hosts did not differ significantly from PBS controls, mice exhibiting decreased pigmentation did exhibit significantly reduced brain weight (Fig. 4D). This reveals the possibility that ^{hi}T cells elicit coordinated age-related degeneration in multiple tissues that express their cognate antigens. To further validate this, we further examined an age-related characteristic in brains of ^{hi}T-bearing nude mice.

3.4. Neuroinflammation in ^{hi}T-bearing nude mice

Increased neuroinflammation is a feature of aging in both mice and humans (Jurgens and Johnson, 2012; Lourbopoulos et al., 2015). Neuroinflammation is primarily characterized by proliferation of activated, glial fibrillary acidic protein (GFAP)-positive astrocytes, as well as Iba-1-positive microglia, and in some cases lymphocytes such as CD8 T cells (Norden et al., 2016; Cupovic et al., 2016). Given apparent correlation of skin with brain changes in ^{hi}T-bearing B6.Foxn1 mice, we asked if they also exhibited neuroinflammatory alterations. Indeed, GFAP⁺ astrocytes appeared elevated in B6.Foxn1 mice 15 months after injection of CD8 T cells, relative to PBS-injected controls (Fig. 4E, F). This was corroborated by

forebrain Western blots, which showed significantly elevated GFAP signal relative to controls (Fig. 4G). This suggested that ^{hi}T cells in B6.Foxn1 mice mediate increased age-related neuroinflammation relative to age-matched controls. To further examine this possibility and explore its mechanism, we stained brains of B6.Foxn1 hosts injected with CD8 T cells from wild-type (wt-CD8 group), Perforin-1-deficient (PrfKO-CD8 group), or IFN γ -deficient donors (Ifn γ KO-CD8 group) 15 months previously, for CD8 T cells, astrocytes, and microglia. Brains of age-matched B6.Foxn1 littermates injected at the same time with PBS were used as controls (PBS group). Numbers of CD8 T cells were significantly elevated in hippocampus of wt-CD8 group mice (Fig. 5A, B), and these could occasionally be seen interacting with pTau⁺ neural cells (Fig. 5A, wt-CD8 group inset). CD8 T cell counts were not elevated outside of hippocampus in cortex (Fig. 5B). Cortical and hippocampal GFAP⁺ astrocytes (Fig. 5C, D), and activated Iba1⁺ microglia (Fig. 5E, F) were also significantly elevated in wt-CD8 group hippocampus and cortex, relative to PBS controls. Intriguingly, PrfKO-CD8 group mice exhibited no increase in CD8 T cells in any region of brain at 15 months, while Ifn γ KO-CD8 group mice still exhibited a significant increase in brain CD8 T cells relative to controls (Fig. 5A). In this context, neither GFAP⁺ astrocytes nor Iba1⁺ microglia were increased in hippocampus or cortex of PrfKO-CD8 or IFN γ KO-CD8 group mice. This suggests that CD8 T cell persistence in brain and IFN γ cytokine production are necessary for the increased astrocytic and microglial neuroinflammation seen in ^{hi}T-bearing nude mice.

3.5. T cell impact on age- and injury-related neuropathology in wild-type mice

Despite the qualitative impact of ^{hi}T cells on tissue defects in nude mice, it remained unclear whether they could measurably impact tissue pathology in fully immunocompetent wild-type animals, and whether they functionally imparted greater similarity to human aging and/or pathology. Single-impact traumatic (TBI) brain injury promotes a distinct amyloidogenic response in mice and humans (Johnson et al., 2010; Nakagawa et al., 1999, 2000), making it potentially useful in addressing whether uniform promotion of age-related T cell expansion in mice to the degree it predominates in humans, renders pathological responses more human-like as well. We thus split mice into sham or TBI groups, and injected half the mice from each group with CD8 T cells from ^{hi}T-bearing B6.Foxn1 donors immediately after TBI (or sham). Peripheral CD8 T cell profiles were analyzed 3 weeks post-TBI, and markers of T cells, amyloidosis, and related pathology analyzed 10 weeks post-TBI (Fig. 6a–e).

At 10 weeks post-TBI, mice given ^{hi}T cells had higher brain levels of A β _{1–40} than sham or TBI mice, with the former exhibiting the reduction in A β typical of mice (Johnson et al., 2010) (Fig. 6b). While ^{hi}T cells in sham mice did not increase levels of A β _{1–40}, CD8 T cells injected into B6. Foxn1 mice without TBI did exhibit such an increase 15 months later. This suggest that ^{hi}T cells in wild-type mice may induce A β _{1–40} accumulation shortly after an injury occurs, but that B6.Foxn1 do so spontaneously over time. TBI mice injected with ^{hi}T cells also had higher levels of pTau and paired helical filament (PHF), a Tau isoform associated with neurofibrillary tangles and neurodegeneration (Fig. 6c). pTau and PHF were also increased, but to a lesser extent in B6.Foxn1 mice 15 months after injection with CD8 T cells, further supporting neuropathologic similarity between the two strains despite its

distinct induction. A significant decrease in the neuronal marker, NeuN, was also evident in wild-type mice receiving both TBI and ^{hi}T cells, as well in wild-type mice receiving ^{hi}T cells alone, and in B6.Foxn1 mice injected 15 months prior with CD8 T cells (Fig. 6d, e). This is consistent with limited neuronal loss in normal aging (Pannese, 2011), and as such supports age-related tissue pathology mediated by ^{hi}T cells in wild-type, in addition to nude recipients. Given that A β ₁₋₄₀ and pTau were not significantly increased in the brains of wild-type mice receiving only ^{hi}T cells, whereas NeuN loss was, suggests that while ^{hi}T cells may be intrinsically capable of damaging neurons to some extent, accompanying physical injury may be required to induce amyloidosis and tauopathy. Surprisingly, and despite ^{hi}T cells' lack of expansion in wild-type hosts, TBI also promoted an early decrease in the proportion of overall KLRG1⁺ CD8 T cells in the peripheral circulation. Since most of these cells are not derived from donors, this is consistent with ^{hi}T cell presence influencing the retention or migration of related bystander T cells. Although further examination is required to validate the generality of this change, this is consistent with brain injury promoting the efflux of potentially destructive ^{hi}T cells and those of similar phenotypes from blood into affected tissues (Fig. 6f).

4. Discussion

In summary, we induced rapid homeostatic expansion of CD8 T cells by injection into nude hosts, which resulted in uniform expansion of aberrant resident memory T cells in young mice, which we termed “^{hi}T” cells. Surface receptors on ^{hi}T cells, including cytokine and other receptors, as well as specific memory subset markers and binding to PNA lectin, were consistently altered in a manner similar to age-related CD8 T_{RM} populations that dominate the T cell pool in aged humans exclusively (den Braber et al., 2012). ^{hi}T genomic DNA in brain also exhibited similar loss of TCR V β diversity, restricted usage of V β D-J joints, and phenotype identical to brain-resident CD8 T cells that accumulate in aged mice. This indicates that ^{hi}T cells faithfully model phenotypic, genotypic, and functional characteristic of aged CD8 T cells independent of other age-related changes. The advantage of this model is that it renders a particular aspect of aging whose impact is minimal in mice (den Braber et al., 2012), more uniform, more similar to humans, and potentially more impactful on human-specific aspects of pathology. We did not examine other known consequences of age-related CD8 T cell accumulation in mice, including decreased responses to immunotherapy or pathogens (Nikolich-Zugich et al., 2012). Nevertheless, our model represents a critical step toward deconvoluting organismal aging into discrete component processes, while allowing unambiguous assessment of the role of CD8 T cell aging in tissue pathology and aging in general.

Validating the model's potential to identify targetable drivers of age-related tissue pathology, ^{hi}T-bearing nude mice showed enhanced age-related pathology in skin and brain, specifically depigmentation and neuroinflammation (Jurgens and Johnson, 2012; Lourbopoulos et al., 2015; Armenta et al., 2019; Rheins et al., 1986). Enhanced neuroinflammation in particular was found to require sustained presence of CD8 T cells in brain, as well as their fully intact pro-inflammatory function, as genetic knockout of the Perforin-1 gene in donor T cells eliminated their sustained presence in brain, while knockout of the IFN γ gene in donor T cells did not. Nevertheless, both knockouts reduced neuroinflammation to control levels

after CD8 T cell injection. Moreover, brain localization of ^{hi}T cells appeared related to their reactivity to brain antigens, and APP₍₄₇₀₋₄₇₈₎ in particular. Thus, isolating this single age-related process, allowed us to identify targetable drivers of age-related tissue pathology, albeit in a manipulated experimental system. Our model nevertheless provided novel insight into the involvement of cytolytic T cells and their effector functions in age-related damage to multiple non-immune tissues. This is remarkable, as waning immune function is widely accepted to impact general health during aging, but has been implicated only in a limited way to age-related disorders in individual tissues such as heart (Ramos et al., 2017). Our findings thus reveal the possibility that general inhibition of T cell activity, inhibition of pro-inflammatory CD8 T cell effectors such as Perforin-1 and IFN γ , and/or modulation of antigen-specific T cell reactivity could conceivably prevent, treat, or reverse age-related pathologies in multiple, ostensibly non-immune tissues. Such intervention would represent an altogether novel approach to mitigate the effects of aging via adaptive immunotherapy.

Importantly, the impact of ^{hi}T cells was demonstrable in wild-type mice, where they not only enhanced neuropathology after brain injury (TBI), but strikingly rendered the amyloid response to it closer to that in humans (Johnson et al., 2010; Nakagawa et al., 1999, 2000). Specifically, reintroduction of ^{hi}T cells initially generated in nude mice into wild-type hosts led to increased beta-amyloid (A β 1–40), accumulation of phosphorylated and pre-aggregated Tau (PHF), and loss of the neuronal marker, NeuN, 10 weeks after traumatic brain injury (TBI). The amyloid response in particular was distinct from the beta-amyloid decrease normally seen in rodents after single-impact TBI, and more similar to the sustained amyloid increase reported in human TBI patients (Johnson et al., 2010; Scott et al., 2016). Intriguingly, amyloid and tau pathology also arose sporadically in ^{hi}T-bearing nude mice over the course of this experiment. This raises the possibility that ^{hi}T cell introduction may confer sporadic neuropathology relevant to human disorders such as Alzheimer's disease (AD) in this mouse strain. In this context, genetic mutations that guarantee AD in humans fail to recreate its most foundational features in transgenic rodent models. This renders much of AD pathology human-specific. It will thus be interesting to determine whether the ability of ^{hi}T cells to “humanize” a post TBI amyloid response extends to AD pathology more generally, in either genetically-induced or sporadic models.

The pathologies observed in ^{hi}T-bearing nude hosts appeared related to their antigenic reactivity, with recognition of epitopes on skin and brain antigens accompanied by detriments in both tissues. It is conceivable that ^{hi}T or age-related counterparts reactive to distinct tissue antigens may damage other areas of the brain or body. CD8 T cell dysfunction in general may thus be relevant to age-related disorders in distinct tissues, and perhaps to the widespread tissue degeneration observed during aging itself. Systematic elucidation of the full range of tissue antigens recognized by ^{hi}T cells in the context of our model may therefore help clarify the impact of cellular immune dysfunction on aging in general, and identify additional drivers of age-related tissue pathology whose targeting may mitigate the impact of aging on human health.

Supplementary Material

Refer to Web version on PubMed Central for supplementary material.

Acknowledgments

We gratefully acknowledge support in conducting behavioral tests from the Cedars-Sinai Research Institute Biobehavioral Core, and Ms. Hannah Schubloom and Mia Oviatt for excellent administrative support and editing.

Funding

This research was supported in part by NIH grants to RC and CW (R21NS054162 and R21AG033394, respectively), a grant from the Joseph Drown Foundation (CJW), and the Maxine Dunitz Neurosurgical Institute.

Abbreviations

T_{RM}	Resident memory T
TCRVβ	T Cell Receptor beta
App	Amyloid Precursor Protein
Aβ	beta-amyloid
pTau	hyper-phosphorylated tau protein
PHF	paired-helical filament

References

- Ahmed M, Lanzer KG, Yager EJ, Adams PS, Johnson LL, Blackman MA, 2009 Clonal expansions and loss of receptor diversity in the naive CD8 T cell repertoire of aged mice. *J. Immunol* 182, 784–792. [PubMed: 19124721]
- Aifantis I, Buer J, von Boehmer H, Azogui O, 1997 Essential role of the pre-T cell receptor in allelic exclusion of the T cell receptor beta locus. *Immunity* 7, 601–607. [PubMed: 9390684]
- Armenta AM, Henkel ED, Ahmed AM, 2019 Pigmentation disorders in the elderly. *Drugs Aging* 36, 235–245. [PubMed: 30637685]
- Buchholz VR, Neuenhahn M, Busch DH, 2011 CD8+ T cell differentiation in the aging immune system: until the last clone standing. *Curr. Opin. Immunol* 23, 549–554. [PubMed: 21664807]
- Clambey ET, van Dyk LF, Kappler JW, Marrack P, 2005 Non-malignant clonal expansions of CD8+ memory T cells in aged individuals. *Immunol. Rev* 205, 170–189. [PubMed: 15882353]
- Clambey ET, White J, Kappler JW, Marrack P, 2008 Identification of two major types of age-associated CD8 clonal expansions with highly divergent properties. *Proc Natl Acad Sci U S A* 105, 12997–13002. [PubMed: 18728183]
- Cupovic J, Onder L, Gil-Cruz C, Weiler E, Caviezel-Firner S, Perez-Shibayama C, Rüllicke T, Bechmann I, Ludewig B, 2016 Central nervous system stromal cells control local CD8(+) t cell responses during virus-induced neuroinflammation. *Immunity* 44, 622–633. [PubMed: 26921107]
- Degauque N, Boeffard F, Foucher Y, Ballet C, Brouard S, Soullillou JP, 2011 The blood of healthy individuals exhibits CD8 T cells with a highly altered TCR Vb repertoire but with an unmodified phenotype. *PLoS One* 6, e21240. [PubMed: 21738624]
- den Braber I, Mugwagwa T, Vrisekoop N, Westera L, Mogling R, de Boer AB, Willems N, Schrijver EH, Spierenburg G, Gaiser K, Mul E, Otto SA, Ruiters AF, Ackermans MT, Miedema F, Borghans JA, de Boer RJ, Tesselaar K, 2012 Maintenance of peripheral naive T cells is sustained by thymus output in mice but not humans. *Immunity* 36, 288–297. [PubMed: 22365666]
- Duong H, Han M, 2013 A multispectral LED array for the reduction of background autofluorescence in brain tissue. *J. Neurosci. Methods* 220, 46–54. [PubMed: 23994358]
- Fonseca R, Beura LK, Quarnstrom CF, Ghoneim HE, Fan Y, Zebley CC, Scott MC, Fares-Frederickson NJ, Wijeyesinghe S, Thompson EA, Borges da Silva H, Vezyz V, Youngblood B,

- Masopust D, 2020 Developmental plasticity allows outside-in immune responses by resident memory T cells. *Nat. Immunol* 21, 412–421. [PubMed: 32066954]
- Gärtner F, Alt FW, Monroe R, Chu M, Sleckman BP, Davidson L, Swat W, 1999 Immature thymocytes employ distinct signaling pathways for allelic exclusion versus differentiation and expansion. *Immunity* 10, 537–546. [PubMed: 10367899]
- Gebhardt T, Mackay LK, 2012 Local immunity by tissue-resident CD8(+) memory T cells. *Front. Immunol* 3, 340. [PubMed: 23162555]
- Johnson VE, Stewart W, Smith DH, 2010 Traumatic brain injury and amyloid-beta pathology: a link to Alzheimer's disease? *Nat. Rev. Neurosci* 11, 361–370. [PubMed: 20216546]
- Jurgens HA, Johnson RW, 2012 Dysregulated neuronal-microglial cross-talk during aging, stress and inflammation. *Exp. Neurol* 233, 40–48. [PubMed: 21110971]
- LeMaout J, Messaoudi I, Manavalan JS, Potvin H, Nikolich-Zugich D, Dyal R, Szabo P, Weksler ME, Nikolich-Zugich J, 2000 Age-related dysregulation in CD8 T cell homeostasis: kinetics of a diversity loss. *J. Immunol* 165, 2367–2373. [PubMed: 10946259]
- Lourbopoulos A, Erturk A, Hellal F, 2015 Microglia in action: how ageing and injury can change the brain's guardians. *Front. Cell. Neurosci* 9.
- Mackay LK, Stock AT, Ma JZ, Jones CM, Kent SJ, Mueller SN, Heath WR, Carbone FR, Gebhardt T, 2012 Long-lived epithelial immunity by tissue-resident memory T (TRM) cells in the absence of persisting local antigen presentation. *Proc. Natl. Acad. Sci. U. S. A* 109, 7037–7042. [PubMed: 22509047]
- Messaoudi I, Lemaout J, Guevara-Patino JA, Metzner BM, Nikolich-Zugich J, 2004 Age-related CD8 T cell clonal expansions constrict CD8 T cell repertoire and have the potential to impair immune defense. *J. Exp. Med* 200, 1347–1358. [PubMed: 15545358]
- Messaoudi I, Warner J, Nikolich-Zugich D, Fischer M, Nikolich-Zugich J, 2006 Molecular, cellular, and antigen requirements for development of age-associated T cell clonal expansions in vivo. *J. Immunol* 176, 301–308. [PubMed: 16365422]
- Morley JK, Batliwalla FM, Hingorani R, Gregersen PK, 1995 Oligoclonal CD8+ T cells are preferentially expanded in the CD57+ subset. *J. Immunol* 154, 6182–6190. [PubMed: 7538544]
- Nakagawa Y, Nakamura M, McIntosh TK, Rodriguez A, Berlin JA, Smith DH, Saatman KE, Raghupathi R, Clemens J, Saido TC, Schmidt ML, Lee VM, Trojanowski JQ, 1999 Traumatic brain injury in young, amyloid-beta peptide overexpressing transgenic mice induces marked ipsilateral hippocampal atrophy and diminished Abeta deposition during aging. *J. Comp. Neurol* 411, 390–398. [PubMed: 10413774]
- Nakagawa Y, Reed L, Nakamura M, McIntosh TK, Smith DH, Saatman KE, Raghupathi R, Clemens J, Saido TC, Lee VM, Trojanowski JQ, 2000 Brain trauma in aged transgenic mice induces regression of established abeta deposits. *Exp. Neurol* 163, 244–252. [PubMed: 10785464]
- Nikolich-Zugich J, Li G, Uhrlaub JL, Renkema KR, Smithey MJ, 2012 Age-related changes in CD8 T cell homeostasis and immunity to infection. *Semin. Immunol* 24, 356–364. [PubMed: 22554418]
- Norden DM, Trojanowski PJ, Villanueva E, Navarro E, Godbout JP, 2016 Sequential activation of microglia and astrocyte cytokine expression precedes increased Iba-1 or GFAP immunoreactivity following systemic immune challenge. *Glia* 64, 300–316. [PubMed: 26470014]
- Onyema OO, Njemini R, Bautmans I, Renmans W, De Waele M, Mets T, 2012 Cellular aging and senescence characteristics of human T-lymphocytes. *Biogerontology* 13, 169–181. [PubMed: 22102004]
- Pannese E, 2011 Morphological changes in nerve cells during normal aging. *Brain Struct. Funct* 216, 85–89. [PubMed: 21431333]
- Park CO, Kupper TS, 2015 The emerging role of resident memory T cells in protective immunity and inflammatory disease. *Nat. Med* 21, 688–697. [PubMed: 26121195]
- Posnett DN, Sinha R, Kabak S, Russo C, 1994 Clonal populations of T cells in normal elderly humans: the T cell equivalent to “benign monoclonal gammopathy” [published erratum appears in *J Exp Med* 1994 Mar 1;179(3):1077]. *J. Exp. Med* 179, 609–618. [PubMed: 8294871]
- Posnett DN, Yarilin D, Valiando JR, Li F, Liew FY, Weksler ME, Szabo P, 2003 Oligoclonal expansions of antigen-specific CD8+ T cells in aged mice. *Ann. N. Y. Acad. Sci* 987, 274–279. [PubMed: 12727652]

- Puig KL, Floden AM, Adhikari R, Golovko MY, Combs CK, 2012 Amyloid precursor protein and proinflammatory changes are regulated in brain and adipose tissue in a murine model of high fat diet-induced obesity. *PLoS One* 7, e30378. [PubMed: 22276186]
- Puig KL, Brose SA, Zhou X, Sens MA, Combs GF, Jensen MD, Golovko MY, Combs CK, 2017 Amyloid precursor protein modulates macrophage phenotype and diet-dependent weight gain. *Sci. Rep* 7, 43725. [PubMed: 28262782]
- Ramos GC, van den Berg A, Nunes-Silva V, Weirather J, Peters L, Burkard M, et al., 2017 Myocardial aging as a T-cell-mediated phenomenon. *Proc. Natl. Acad. Sci. U. S. A* 114, E2420–E2429. [PubMed: 28255084]
- Rheins LA, Palkowski MR, Nordlund JJ, 1986 Alterations in cutaneous immune reactivity to dinitrofluorobenzene in graying C57BL/vi.vI mice. *J. Invest. Dermatol.* 86, 539–542. [PubMed: 3462262]
- Ricalton NS, Robertson C, Norris JM, Rewers M, Hamman RF, Kotzin BL, 1998 Prevalence of CD8+ T-cell expansions in relation to age in healthy individuals. *J. Gerontol. A Biol. Sci. Med. Sci* 53, B196–203. [PubMed: 9597044]
- Ritzel RM, Crapser J, Patel AR, Verma R, Grenier JM, Chauhan A, Jellison ER, McCullough LD, 2016 Age-Associated Resident Memory CD8 T Cells in the Central Nervous System Are Primed To Potentiate Inflammation after Ischemic Brain Injury. *J. Immunol* 196, 3318–3330. [PubMed: 26962232]
- Rodriguez-Garcia M, Fortier JM, Barr FD, Wira CR, 2018 Aging impacts CD103(+) CD8(+) T cell presence and induction by dendritic cells in the genital tract. *Aging Cell* 17, e12733. [PubMed: 29455474]
- Schenkel JM, Fraser KA, Vezyz V, Masopust D, 2013 Sensing and alarm function of resident memory CD8⁺ T cells. *Nat. Immunol* 14, 509–513. [PubMed: 23542740]
- Schwab R, Szabo P, Manavalan JS, Weksler ME, Posnett DN, Pannetier C, Kourilsky P, Even J, 1997 Expanded CD4⁺ and CD8⁺ T cell clones in elderly humans. *J. Immunol* 158, 4493–4499. [PubMed: 9127016]
- Scott G, Ramlackhansingh AF, Edison P, Hellyer P, Cole J, Veronese M, Leech R, Greenwood RJ, Turkheimer FE, Gentleman SM, Heckemann RA, Matthews PM, Brooks DJ, Sharp DJ, 2016 Amyloid pathology and axonal injury after brain trauma. *Neurology*.
- Smolders J, Remmerswaal EB, Schuurman KG, Melief J, Van Eden CG, Van Lier RA, Huitinga I, Hamann J, 2013 Characteristics of differentiated CD8(+) and CD4 (+) T cells present in the human brain. *Acta Neuropathol.* 126, 525–535. [PubMed: 23880787]
- Wakim LM, Woodward-Davis A, Bevan MJ, 2010 Memory T cells persisting within the brain after local infection show functional adaptations to their tissue of residence. *Proc. Natl. Acad. Sci. U. S. A* 107, 17872–17879. [PubMed: 20923878]
- Wakim LM, Woodward-Davis A, Liu R, Hu Y, Villadangos J, Smyth G, Bevan MJ, 2012 The molecular signature of tissue resident memory CD8 T cells isolated from the brain. *J. Immunol* 189, 3462–3471. [PubMed: 22922816]
- Zlomy M, Almanzar G, Parson W, Schmidt C, Leierer J, Weinberger B, Jeller V, Unsinn K, Eyrich M, Wurzner R, Prelog M, 2016 Efforts of the human immune system to maintain the peripheral CD8+ T cell compartment after childhood thymectomy. *Immun. Ageing* 13, 3. [PubMed: 26839574]

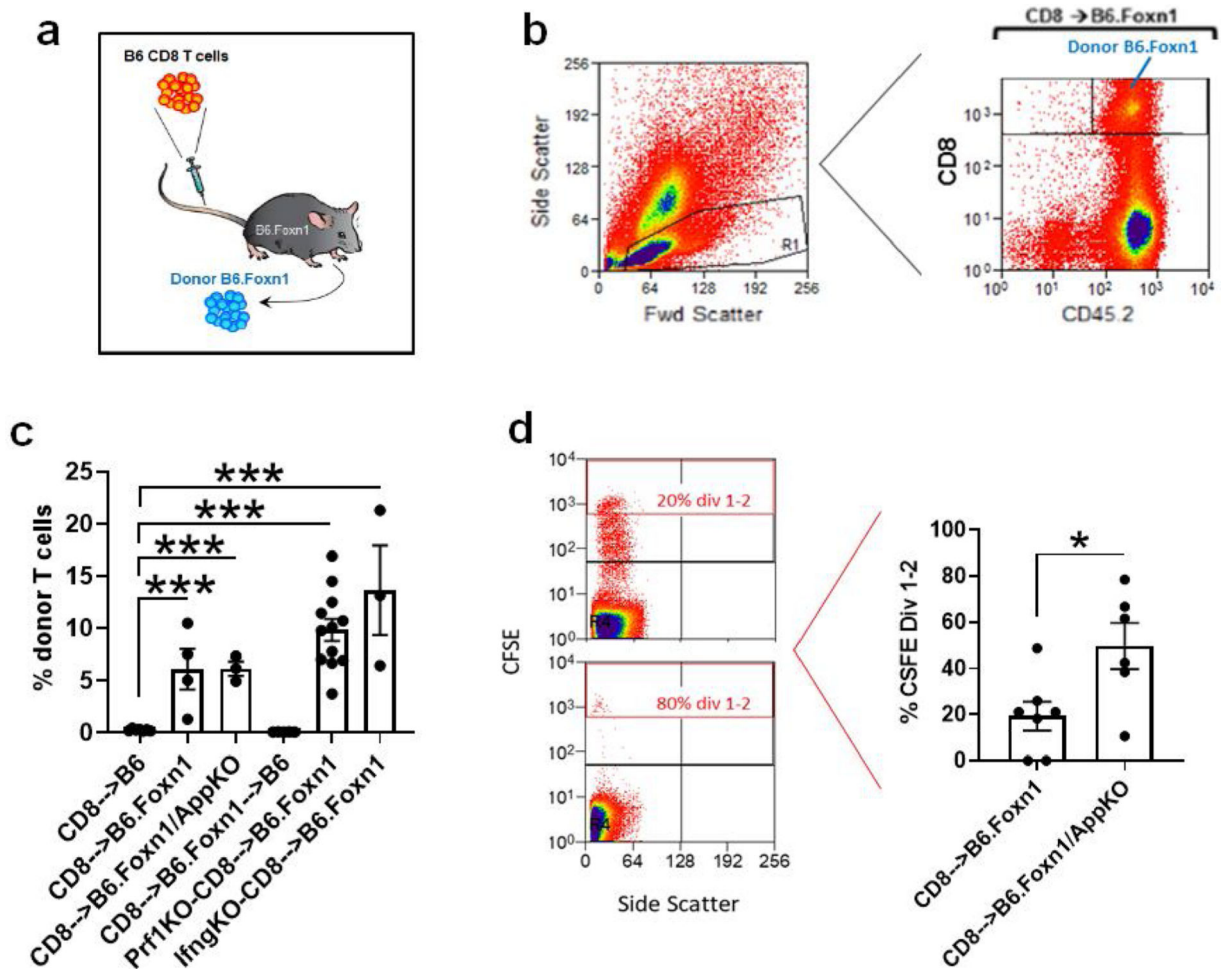


Fig. 1. Expansion of donor CD8 T cells in mouse recipients.

Purified CD8 T cells from female C57BL/6, B6.CD45.1-congenic (B6 recipients only; CD8→B6), or congenic effector knockout hosts (Perforin-1- or Ifn γ -deficient), or from previously injected B6.Foxn1 donors, were injected into 8–10 week-old female C57BL/6 J, B6.Foxn1, or B6.Foxn1/AppKO, recipients as indicated (A). Blood was analyzed by flow cytometry 5–8 days later using the gating and antibodies to T cell markers as shown (B), with % CD3 ϵ ⁺CD8⁺ in gated donor cells compiled in (C), where “% donor T cells” refers to the percent donor T cells within gated recipient lymphocytes. Note that both B6.Foxn1 mice and C57BL/6 are CD45.2. Fig. 1B depicts lymphocytes from CD45.2⁺ donors in CD45.2⁺ B6.Foxn1, and thus contains plentiful non-T lymphocytes. B6.Foxn1 mice were crossed to B6.App-knockout mice, homozygous double-mutants (B6.Foxn1/AppKO) verified by PCR and phenotype at Jackson Laboratories (Bar Harbor, MN). Purified CD8 T cells were labeled with CFSE, and their expansion assessed by CFSE dilution in B6.Foxn1 and B6.Foxn1/AppKO female recipients (D; n = 3 B6.Foxn1 & n = 5 B6.Foxn1/AppKO; **P* < 0.04, ****P* < 0.00001 by 2-tailed T-test in ≥ 3 independent tests for all markers).

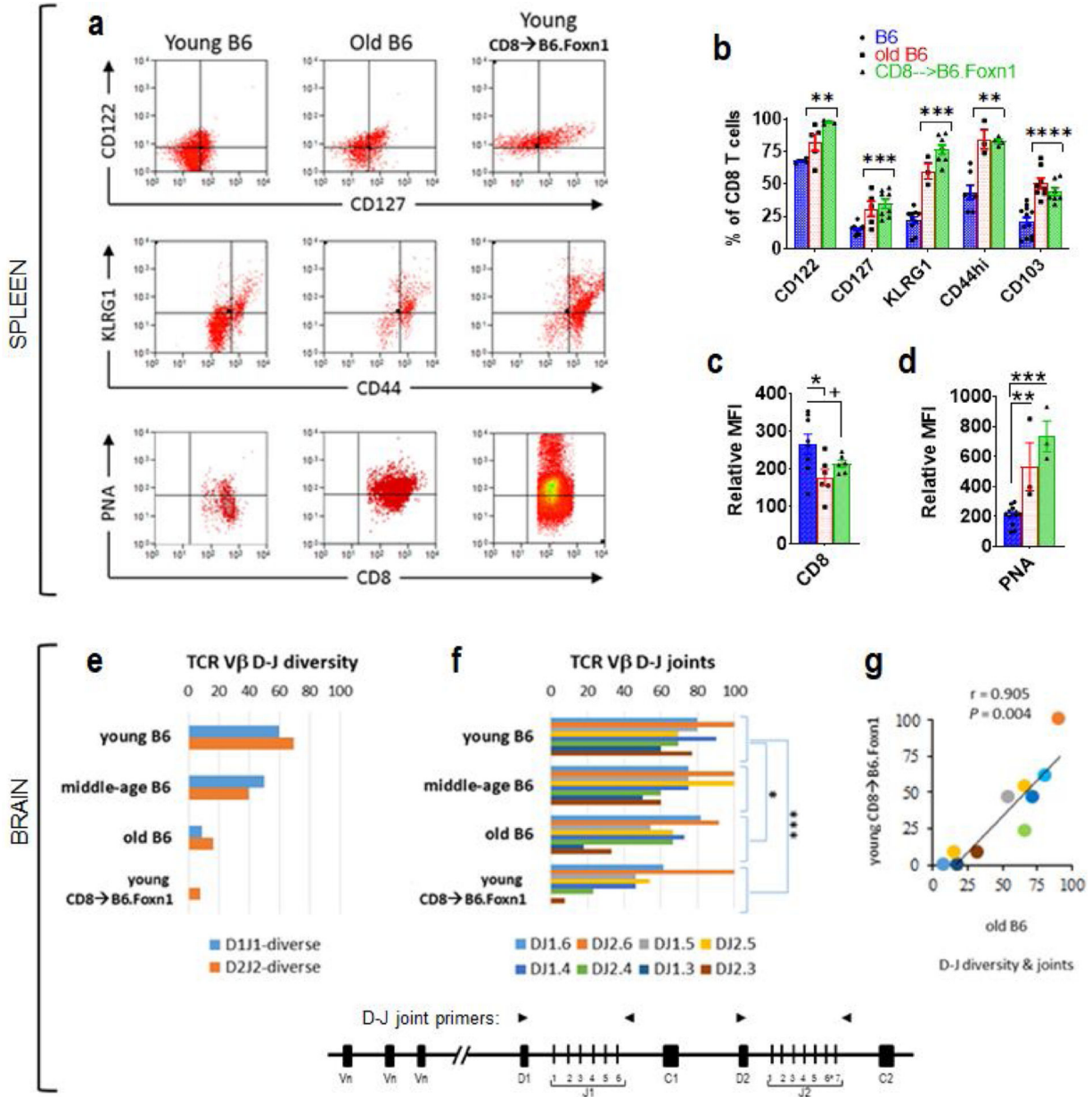


Fig. 2. Age-related hiT cell phenotype in young mice.

Representative flow cytometry analysis of age-related markers on splenic CD8 T cells from young (< 10 weeks) and old (> 12 months) C57BL/6 (B6), and young (6 weeks) B6.Foxn1 recipients of i.v. CD8 T cells (CD8→B6.Foxn1) 3–5 weeks after injection (A). Antibody combinations used were: CD3 PEcy5, CD8 PE, CD4 FITC (control, not shown); CD8 PECy5, CD122 FITC, CD127 PE, CD45.2 PacBlue (top panel); CD8 FITC, CD44 PE, KLRG1 Biotin/SACy, CD45.2 PacBlue (2nd panel); CD8 FITC, PNA APC (3rd panel); CD8 PacBlue, CD103 FITC (4th panel). Percentage of lymphocytes (B) and mean fluorescence intensity (C, D) from flow cytometry compiled from $n \geq 6$ mice/group. **T cell receptor (TCR) gene segment usage and diversity in nude mice harboring hiT_{RM}.** Proportions of mice with “diverse” TCR $\nu\beta$ D→J gene segment usage (> 3 segments/brain)

and specific D→J segments within brains of young (<10 weeks), middle-aged (6 months), and old (> 12 months) B6 mice, reveals an age-dependent pattern of progressively decreased diversity and increased usage of particular D→J segments (i.e., clonality; **E, F**). D→J diversity and segment usage was significantly correlated only between old B6 and young CD8→B6.Foxn1 brain; colors for specific D-J joints are derived from E & F (**G**). Schematic of forward (right-facing arrowhead) and reverse (left-facing arrowhead) TCRβ locus D1-J1 and D2-J2 primers is depicted beneath E-F. Additional detail and representative gels are provided in Supplemental Fig. S1. * $P < 0.05$, ** $P < 0.01$, *** $P < 0.005$ by 2-sided T-test relative to B6 for flow cytometric markers, and by Pearson's correlations in $n \geq 10$ mice/group for PCR compilations.

Author Manuscript

Author Manuscript

Author Manuscript

Author Manuscript

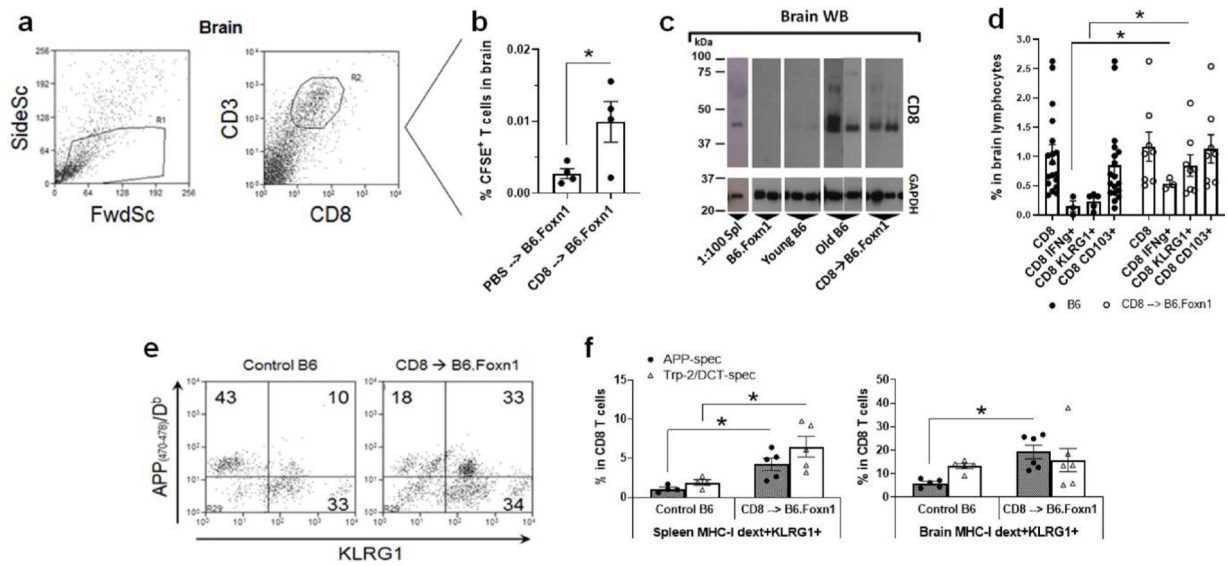


Fig. 3. Brain CD8 T cell phenotype after transfer into nude mice.

Light scatter and gating of brain lymphocytes and CD8 T cells in B6.Foxn1 recipients (A). Percentage and phenotype of CFSE⁺ CD8 T cells within brain lymphocytes in B6.Foxn1 recipients 3 days (B). Western blot of CD8 α (antibody clone 2.43; (C) in dissected brain hippocampus of young (<5 months) C57BL/6 (B6) and B6.Foxn1 hosts with and without adoptive transfer of CD8 T cells from young (6–8 wk) B6 donors 10 weeks prior. 1:100 Spl = 6–10 week-old female C57BL/6 splenocyte lysate, diluted 1:100 relative to brain, and subjected to identical analysis. Phenotype of brain-resident CD8 T cells, compiled from ≥ 5 wild-type B6 or CD8 T cell-injected B6.Foxn1 mice, injected 10 weeks prior (D). Increased staining with pMHC I multimers (custom dextramers synthesized by Immudex USA, Fairfax, VA) to Trp-2-DCT_{(180–188)/H-2K^b} and APP_{(470–478)/H-2D^b} epitopes on KLRG1⁺ CD8 T cells in B6.Foxn1 brain (E, F) and spleen (F), 10 weeks after injection (* $P < 0.05$ by 2-sided T-test in ≥ 3 independent tests; $n > 6$ for all analyses, with significance relative to PBS group).

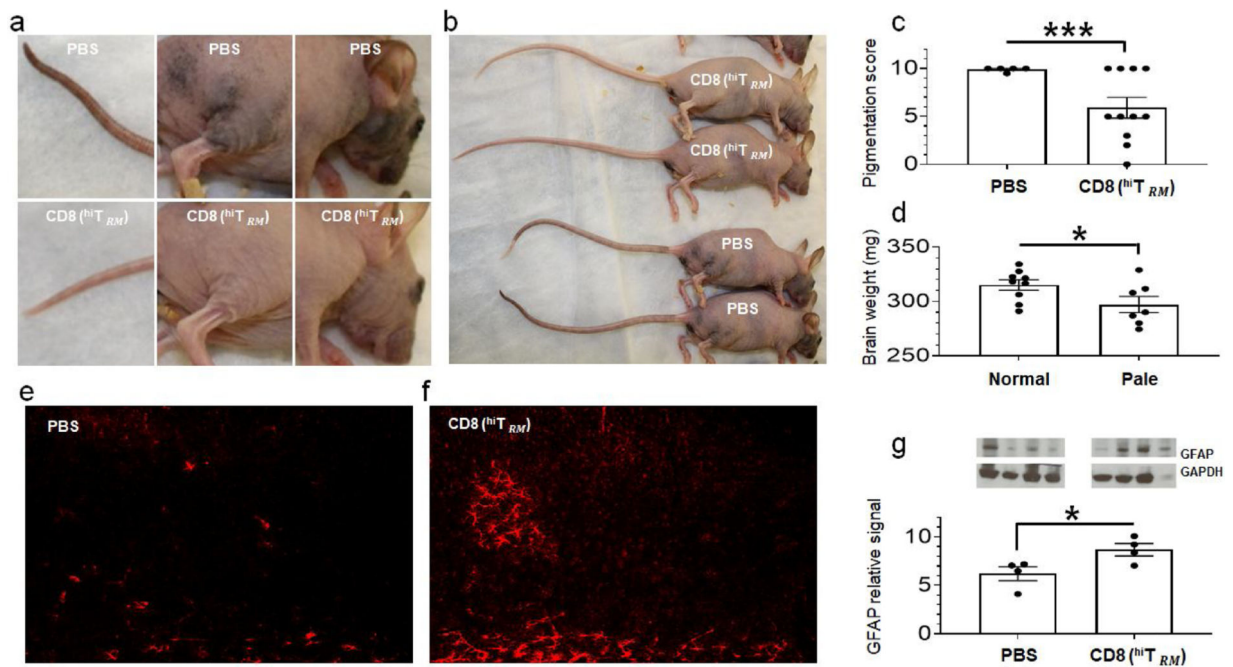


Fig. 4. Age-related skin and brain pathology in hiT_{RM} -bearing nude mice.

Residual pigmentation 15 months after cell or control PBS injection was quantified on a 1–10 scale, with 10 equal to the highest pigmentation, 5 equivalent to roughly $\frac{1}{2}$ the maximum level pigmentation by affected area, 2.5 equivalent to roughly $\frac{1}{4}$ the maximum level, etc. Most mice receiving CD8 T cells (harboring hiT_{RM}) exhibited visibly reduced pigmentation (A, B), and significantly lower pigmentation scores (C). Mice with pigmentation scores < 9 (“pale”) also exhibited significantly lower brain weight than those with higher pigmentation (“normal”; D). Hippocampal brain sections of PBS- or CD8 T cell-injected B6.Foxn1 hosts were stained for GFAP⁺ astrocytes 15 months after injection (E, F), and Western blots performed on forebrains from the same groups and time points, with GFAP signal quantified relative to control GAPDH (G). * $P < 0.05$, ** $P < 0.01$, *** $P < 0.005$ by 2-sided T-test in ≥ 3 independent tests for all analyses relative to PBS group, except brain weight, for which 1-sided T-tests were performed.

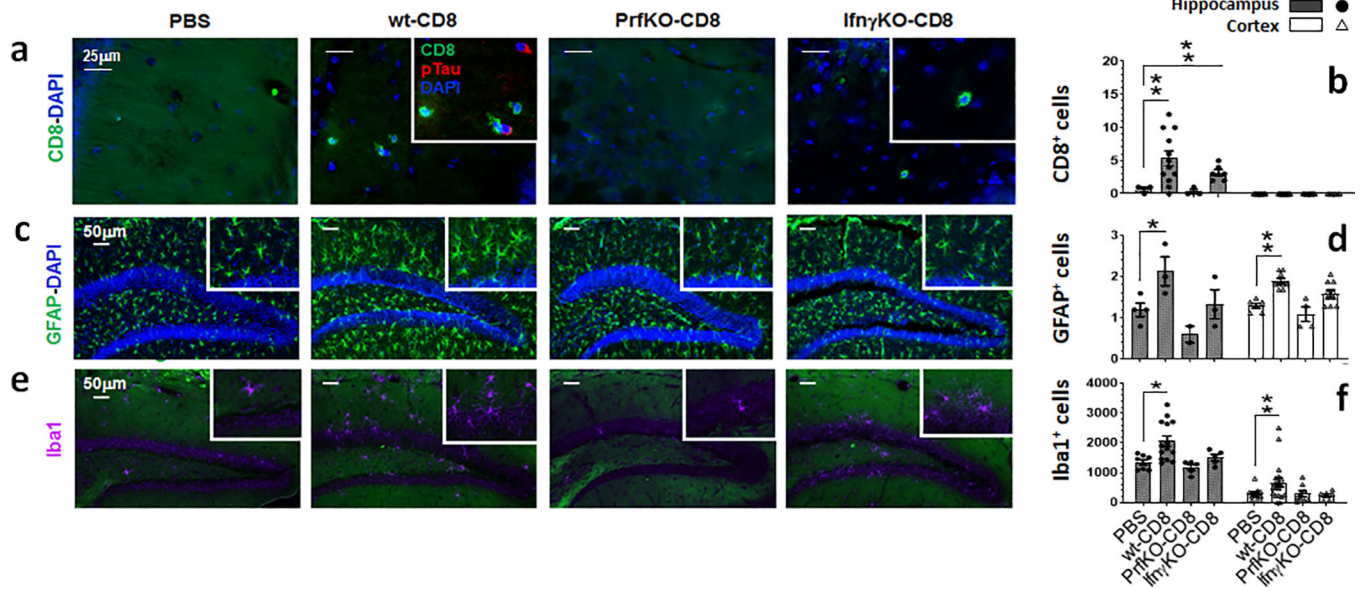


Fig. 5. Mechanistic requirements of neuroinflammation in $hiTRM$ -bearing nude mice. Brain was co-stained for CD8 and pTau (inset) (A), and quantified within hippocampal and cortical brain sections from B6.Foxn1 recipients 15 months after injection of wild-type, Ifn γ KO or PrfKO CD8 T cells, or PBS. CD8⁺ cells, though mostly solitary, were occasionally seen interacting with pTau⁺ neurons as in A (inset). Group data are compiled in (B). Images and compilations of GFAP⁺ astrocytes (C, D), and Iba1⁺ microglia (E, F). * $P < 0.05$, ** $P < 0.01$, *** $P < 0.005$ by 2-sided T-test in ≥ 3 independent tests for all analyses, relative to PBS group.

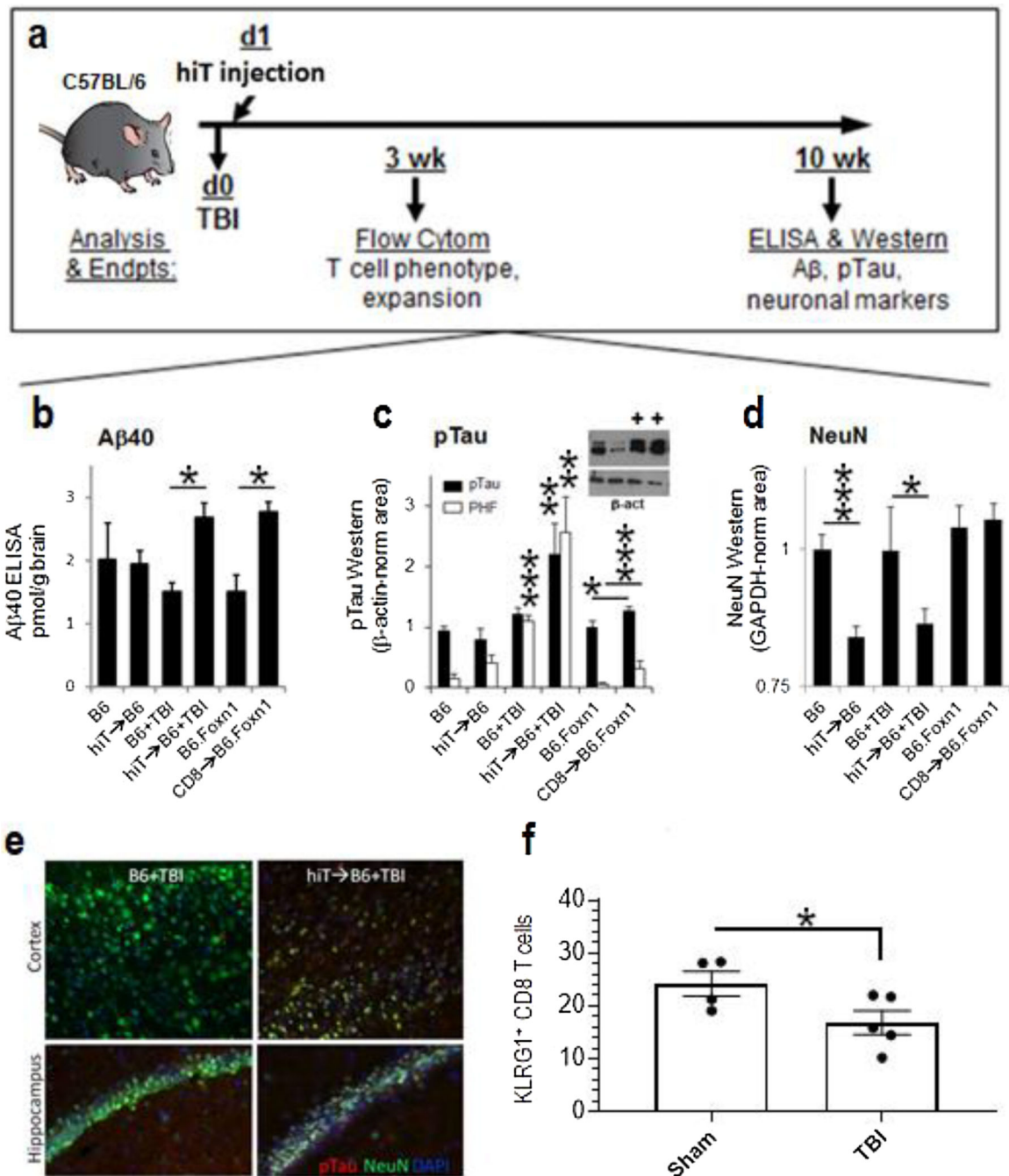


Fig. 6. Synergy between hiT cells and brain injury in wild-type mice.

Pre-prepared hiT cells were injected into 10-wk wild-type (B6) brain- (TBI) or sham-injured females. Mice were bled on 1 day and 3 weeks after hiT cell injection, and sacrificed at 10 wk (A). Forebrain ELISA of Triton-soluble mouse A β 1–40 (A), pTau/PHF (B), and NeuN Western blot signal (C), in B6 recipients (n = 6/: “+” above pTau bands = hiT cell recipients), with pTau and NeuN trends confirmed by tissue IF staining (D). Flow cytometric analysis of CFSE⁺ hiT cells performed 1 day after cell injection (F). Note that the endpoint

of analysis of the B6.Foxn1 groups is 15 months post-injection (control or CD8 T cell). * $P < 0.05$, *** $P < 0.005$, in two-sided T -test.

Author Manuscript

Author Manuscript

Author Manuscript

Author Manuscript